 Bull. Chem. Soc. Jpn., 74, 2151–2160 (2001)

Highly Enantioselective Cyclopropanation of Styrenes and Diazoacetates Catalyzed by 3-Oxobutylideneaminatocobalt(II) Complexes, Part 2. Semiempirical Analysis of Diastereo and Enantioselectivities

Taketo Ikeno, Izumi Iwakura, and Tohru Yamada*

Department of Chemistry, Faculty of Science and Technology, Keio University, Hiyoshi, Kohoku-ku, Yokohama 223-8522

(Received March 13, 2001)

A semiempirical analysis using the PM3(tm) method was performed on the 3-oxobutylideneaminatocobalt(II) complexes-catalyzed cyclopropanation. Although the energy diagram calculated by the PM3(tm) method had a contradiction, where the product was less stable than the reactant, the structures and the energies of the reactant and the transition state obtained by the PM3(tm) method could be relatively reliable by comparing with the results based on the density functional theory. Analysis of the transition states by the PM3(tm) method indicated that the olefin approached parallel to the cobalt-carbene bond with bisecting an O_1–Co–O_2 angle. It was revealed that the transition state affording the (1*S*,2*S*)-arylcyclopropanecarboxylic acid ester corresponding to the (1*S*,2*S*)-cobalt complex was the most stable, because of the lowest steric repulsion among the aryl group of the diamine unit, the ester moiety, and the approaching olefin. It was clarified that the enantioselectivity occurred due to the repulsion between the aryl group of the diamine unit and the ester moiety and that the diastereoselectivity was controlled by the repulsion between the ester moiety and the approaching olefin.

Transition metal-catalyzed enantioselective cyclopropanations are now some of the most useful reactions for the synthesis of optically active cyclopropane compounds. They are used for the industrial synthesis of pyrethroid and Cilastatin, and a variety of ligands for transition-metal complexes are being developed both in laboratories and in industries. Copper(I) complexes with Schiff base,[1] semicorrin,[2] bis(oxazoline)[3] or bipyridine[4] ligands, ruthenium(II) complexes with 2,6-di(2-oxazolin-2-yl)pyridine[5] ligands, and rhodium(III) complexes with chiral carboxamidate[6] and carboxylate[7] ligands were developed as effective catalysts to provide an extremely high level of enantioselectivity. Optically active (dioximato)cobalt(II),[8] (salen)cobalt(II) and (III),[9] and 3-oxobutylideneaminatocobalt(II)[10] complexes were efficient catalysts for the asymmetric cyclopropanation of styrenes. In spite of the many previously reported varieties of transition-metal catalysts, discussions of the precise mechanism of these reactions were seldom reported and only several transition-state models have been proposed, based on the reactivity of the substrates, the absolute configuration and diastereo-/enantioselectivity of the product. For the copper-Schiff base-catalyzed cyclopropanation,[1] it was proposed that the metallacyclobutane intermediate **1** was first generated from the copper-carbene complex and olefin and the following reductive elimination gave the product (Fig. 1). A similar cobaltacyclobutane intermediate was also proposed for the enantioselective cyclopropanation catalyzed by the (dioximato)cobalt(II) complex.[8] It was postulated that the olefin approached parallel to the cobalt-carbenoid to produce cobaltacyclobutane **2** and that cyclopropane was obtained via this intermediate.

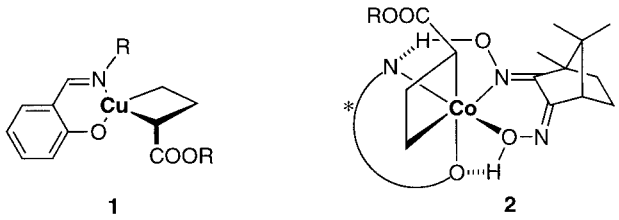

1 **2**

Fig. 1. Proposed metallacyclobutane intermediates.

Contrary to the metallacyclobutane intermediate, the concerted mechanisms were recently proposed for the enantioselective cyclopropanation reactions catalyzed by the transition-metal complexes. As shown in Scheme 1, it was considered that the olefin approached the metal–carbene intermediate and that the corresponding cyclopropane was produced by releasing the transition-metal complex through a three-centered transition state.

In concerted mechanisms, however, the various approaching trajectories of olefins should be considered. For examples, it was proposed that the olefin perpendicularly approached the metal–carbene bond in the cobalt(III)-salen catalyzed cyclopropanation (Fig. 2, **3**),[9b] while a parallel approach of the olefin to the metal–carbene bond was proposed for the copper(I)–semicorrin[2] and ruthenium(II)–pybox[5] catalyzed cyclopropanations (Fig. 2, **4**). The concerted mechanisms for the rhodium complex-catalyzed cyclopropanations were quite disputed; for the intermolecular cyclopropanation using tetrakis[methyl (*S*)-5-oxo-κO-pyrrolidine-5-κN-2-carboxylate]dirhodium(Rh-Rh)(II)[6b] or tetrakis[(*S*)-3-phthalimido-2-piperidinonate-

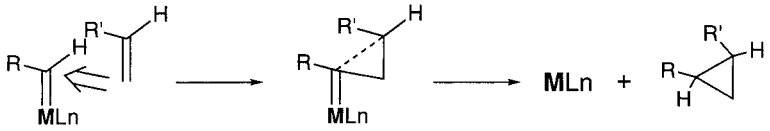

Scheme 1. Concerted mechanism of the cyclopropanation.

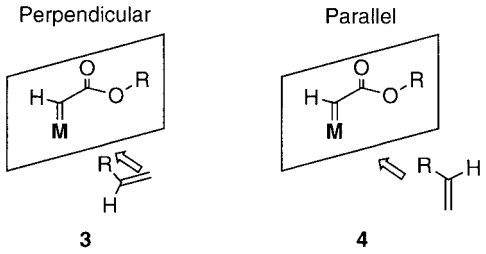

Fig. 2. Orientations of the approaching olefin.

$\kappa N,\kappa O$]dirhodium(Rh-Rh)(II)[6c] as a catalyst, parallel approaches of the olefin to the rhodium-carbene bond were consistent with the absolute configuration of the product (Fig. 2, **4**); on the contrary, perpendicular approaches were postulated for the cyclopropanation[11] by rhodium(III) porphyrin and for the cyclopropanation of vinylcarbenoid[7] by tetrakis[1-[4-*tert*-butylphenyl]sulfonyl]-(2*S*)-pyrrolidinecarboxylate]dirhodium (Fig. 2, **3**). For the intramolecular cyclopropanations catalyzed by the copper-bisoxazoline or rhodium complexes, it was suggested that an olefin approached in a parallel, perpendicular, or skew orientation according to the respective structures of the substrates and the catalysts.[12]

As described above, the mechanisms of the transition-metal catalyzed cyclopropanations were not fully understood and the proposals for the intermediate and the trajectory of the olefin just explained the structure of the products. Besides, theoretical investigations for the mechanisms and transition states have been performed only on a limited basis[13] despite the fact that molecular orbital calculations are today successfully applied to analysis of various transition-metal catalyzed reactions. It should be expected that the theoretical studies on the mechanism and transition state will provide pertinent information for design of excellent ligands and catalysts. In this paper, we report the analysis of the transition states of the enantioselective cyclopropanation catalyzed by the 3-oxobutylideneaminatocobalt(II) complex and present some plausible explanations for the diastereo- and enantioselectivities of the reaction.

Computational Method

Semiempirical calculations were carried out using the PM3(tm) method[14] implemented in Mac Spartan Pro Ver 1.0.1 and PC Spartan Pro Ver 1.0.[15] The PM3(tm) method was modified from the original PM3 procedure[16] for the calculation including transition metals and recently applied to the theoretical analysis on the structures and energies of the transition metal complexes.[17] The analysis of the cyclopropanation catalyzed by the 3-oxobutylideneaminatocobalt(II) complex was performed using the default parameters supplied by the program Mac Spartan Pro or PC Spartan Pro. Each transition state possesses only one imaginary frequency for the vibrational analysis, corresponding to the appropriate coordinate of the reaction. In order to confirm the applicability of the PM3(tm) parameters for the present catalytic enantioselective cyclopropanations, density functional calculations were carried out using Gaussian 98.[18] Full geometry optimizations were performed at B3LYP/LANL2DZ[19] for the ground states and transition states. The stable calculation revealed the obtained wave functions to be the most stable. The transition state structures possessed only one imaginary frequency and the vibration modes corresponding to the expected c.d.r. An IRC calculation was also performed for the transition structure to confirm that it is the true transition state.

Results and Discussion

An orange-colored solution of the 3-oxobutylideneaminatocobalt(II) complex turned brown with evolving nitrogen immediately after the diazoacetate was added to the solution in the presence of *N*-methylimidazole. It was reported that the ruthenium–carbene complex with the pybox ligand was isolated and its structure was fully determined by an X-ray diffraction analysis.[20] The isolated ruthenium–carbene complex was then reacted with styrene to afford the corresponding optically active cyclopropanecarboxylate. Based on these observations and knowledge, it was reasonable to consider that the cobalt–carbene complex **5** was first generated as a stable intermediate (Fig. 3) and then reacted with styrene to give the corresponding cyclopropane derivative. Also, it should be postulated that the diastereo- and enantioselectivities were regulated during the last step. The PM3(tm) method was first adopted for the analysis of the transition state of the reaction between the cobalt–carbene complex and styrene, because the analysis of the real cobalt complex by ab initio method was too complicated. We planned to confirm the applicability of the parameters for the PM3(tm) Hamiltonian in the model system **6** (Fig. 3) by comparison with the density functional method, and then the analysis by the PM3(tm) method was developed step-by-step for the real cobalt complex system **5**.

We first examined the feasibility of the PM3(tm) parameters for the calculation of the cyclopropanation reaction, since semiempirical methods sometimes result in inadequate predictions for strained compounds and for the transition state. Based on the PM3(tm) method, the transition state for the reaction of the CF_2 carbene and ethylene was obtained as the structure **7** (i = 580 cm^{-1}), in which one bond (1.82 Å) between the carbene and ethylene was shorter than the other bond (2.22 Å) (Fig. 4). It was fairly consistent with a model of the non-least motion pathway by ab initio calculation.[21]

Additionally, no activation barrier was found in the PM3(tm) calculation for the cyclopropanation of the CH_2 carbene with ethylene, nor for the ab initio result by Houk et al.[22] Based on these results, it was reasonable to consider that the PM3(tm) parameters were applicable to the analysis of the cyclopropanation reaction. The transition state calculations of

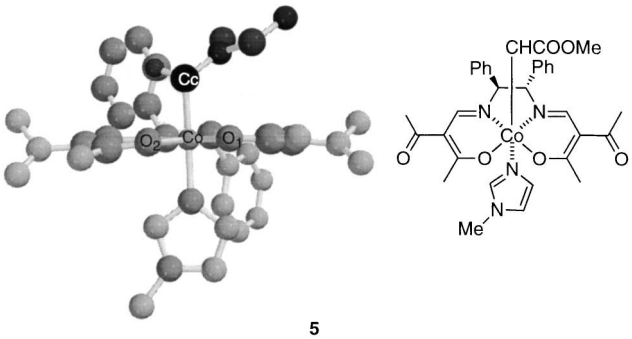

5

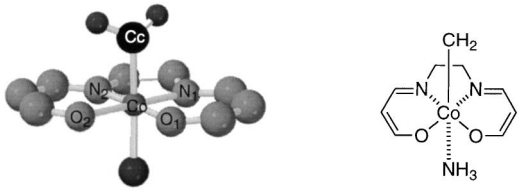

6

Fig. 3. Cobalt carbene intermediate **5** and model cobalt carbene complex **6**.

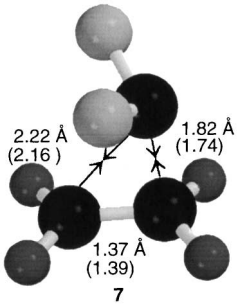

7

Fig. 4. Transition state for the reaction of the CF_2 carbene with ethylene at PM3(tm). Reported structure parameters at HF/3-21G by Houk[21b] were shown in parenthesis.

the model carbene complex **6** and ethylene were then started. The potential energy surfaces along the parallel and perpendicular trajectory of ethylene to the cobalt-carbene with bisecting the O_1–Co–O_2 angle were first calculated. After transition state optimization from the energy maxima of the potential energy surface, the transition structure **8** (i = 672 cm^{-1}) in a parallel orientation and the transition structure **9** (i = 652 cm^{-1}) in a skew orientation were obtained (Fig. 5).

Since transition states were obtained, reaction coordinate was calculated next. As shown in Fig. 6, a contradiction was observed for the reaction coordinate. Compared with the respective energies, the product was less stable than the transition state by 200.7 kJ mol^{-1}.

Although the energy diagram by the PM3(tm) method had a contradiction, their structures and energies of the reactant and transition states were revealed to be reliable by comparing with that by the density functional method. Density functional calculations were subjected to the reactant, the transition state, and the product. Optimization was performed by the B3LYP method with LANL2DZ as a basis set using the structure optimized by the PM3(tm) method as an initial geometry. The

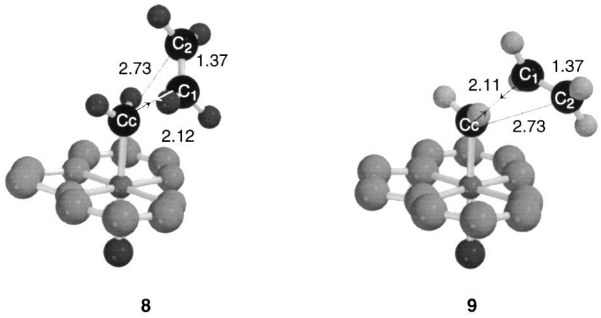

8 9

Fig. 5. Transition states for the reaction of the model cobalt carbene complex **6** with ethylene at PM3(tm).

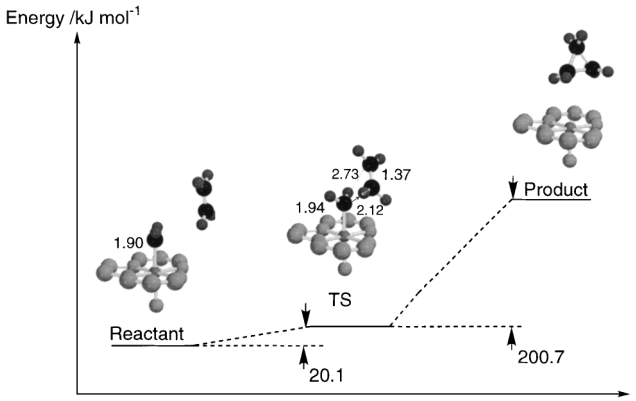

Fig. 6. Potential energy diagrams for the reaction of the cobalt complex **6** with ethylene at PM3(tm)//PM3(tm).

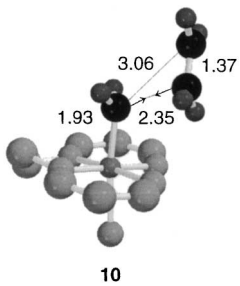

10

Fig. 7. Transition state **10** for the reaction between the cobalt carbene complex **6** and ethylene at B3LYP/LANL2DZ.

transition state structure **10**, in which the olefin approached parallel to the cobalt–carbene bond, was obtained from transition state **8** (Fig. 7).[23] Compared with the optimized structures **8** and **10**, the shapes of the triangle structures resemble each other. Two reaction coordinates were obtained by a single point calculation at the B3LYP/LANL2DZ level using the optimized structure at PM3(tm) (Fig. 8) and fully at the B3LYP/LANL2DZ levels (Fig. 9).

Reasonable potential energy diagrams were obtained, as shown in Fig. 8 and 9, while appropriate activation energies were afforded in each calculation as 20.1 (Fig. 6), 43.7 (Fig. 8), and 22.1 (Fig. 9) kJ mol^{-1}, respectively. These results indicated that the energy difference between the reactant and the transition state was adequately estimated by the PM3(tm) method, whereas the energy of the product could not be pre-

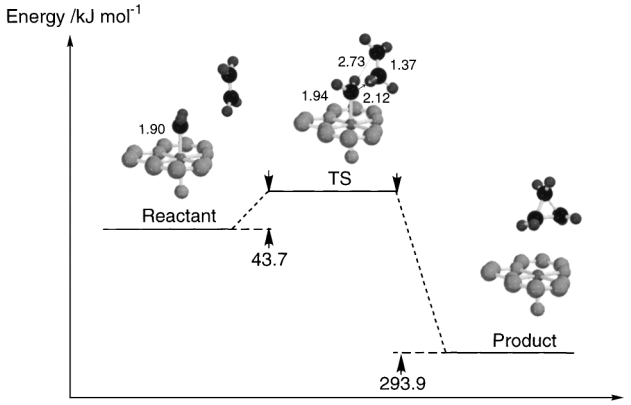

Fig. 8. Potential energy diagrams for the reaction of the cobalt complex **6** with ethylene at B3LYP/LANL2DZ// PM3(tm).

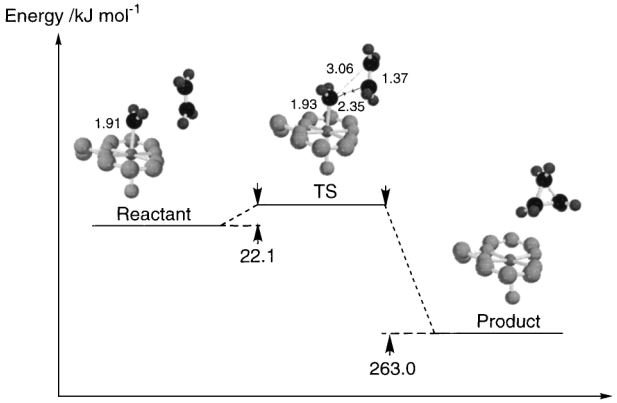

Fig. 9. Potential energy diagram for the reaction of the cobalt complex **6** with ethylene at B3LYP/LANL2DZ// B3LYP/LANL2DZ.

dicted by the PM3(tm) method. This inconsistency could be ascribed to the poor estimation of the energy for the resulting pentadentate Co(II) complex. From these results mentioned above, the activation energy of the present catalytic cyclopropanation was essentially small because of the small steric effect. That is, the transition states should exist during the early stage of the reaction and the organization around the cobalt complex would be little changed by the transition state. Therefore, the estimation error from the coordination change in the cobalt complex was small enough for us to rely on the calculated structure and energy of the transition states.

As we had confirmed that the PM3(tm) parameters were reliable for the ground state and the transition state, a precise analysis of model system **8** was carried out. Based on the obtained transition state **8** and **9**, totally 15 rotational isomers of the transition states were obtained. The most stable isomer **9** among them is shown in Fig. 10 as a representative.[24]

A further detailed analysis of the transition state was per-

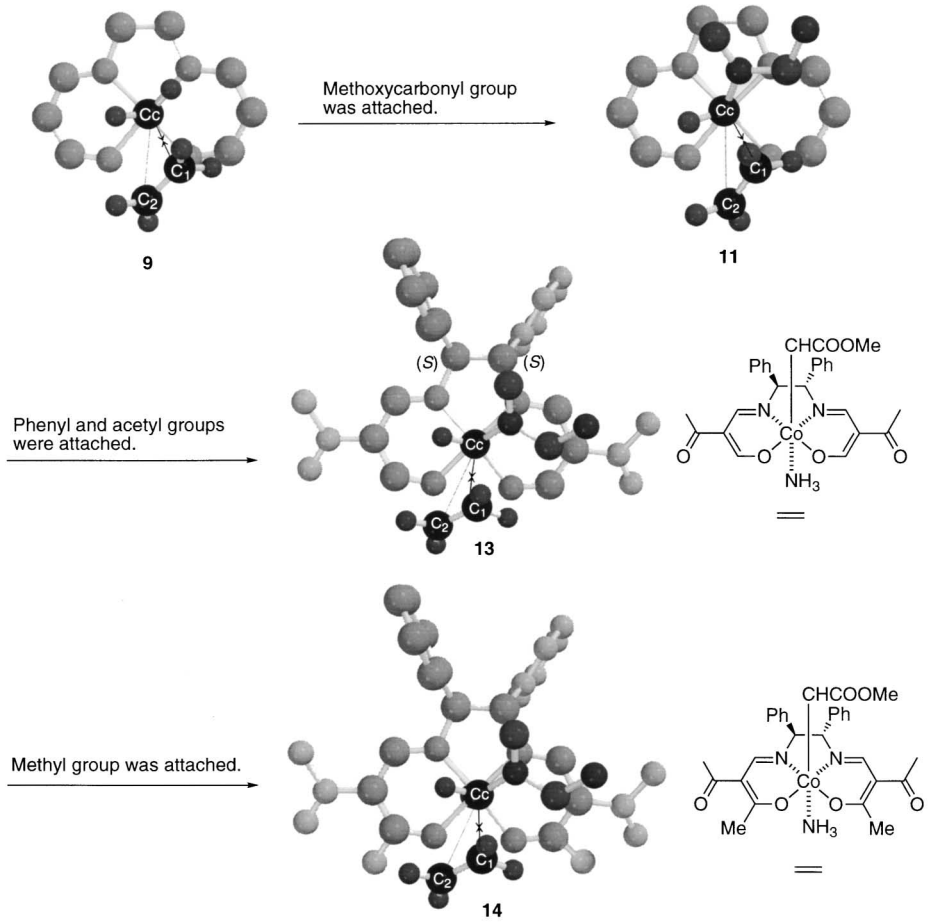

Fig. 10. Developing the model cobalt complex for the real catalyst.

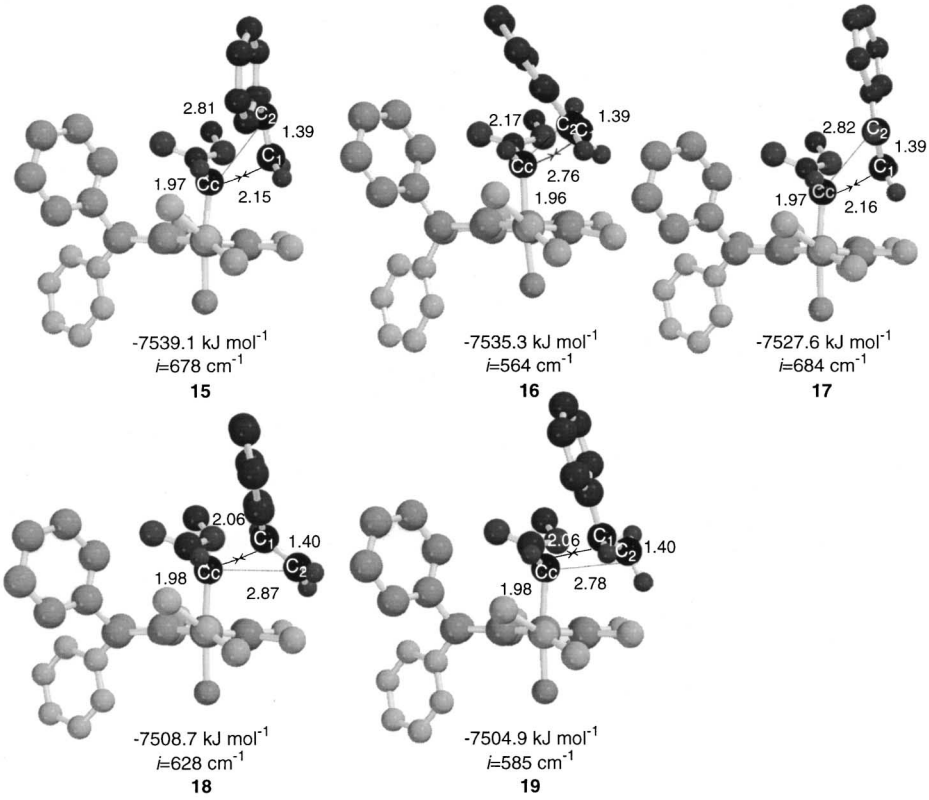

Fig. 11. Various transition states of the reaction between the cobalt carbene complex and styrene.

formed from the above 15 transition states. Hydrogen of CH_2 carbene was replaced with methoxycarbonyl group, and then rotational analysis around the C_c–C_1 and Co–C_c bond afforded 9 transition states. The most stable isomer **11** among them is shown in Fig. 10 as a representative.[25,26]

At the next stage,[27] the phenyl groups were attached on the ethylene bridge of structure **11** in the pseudoequatorial conformations according to the X-ray crystallographic analysis of (1*S*,2*S*)-[*N*,*N*′-bis{2-(2,4,6-trimethylbenzoyl)-3-oxobutylidene}-1,2-diphenylethylenediaminato]cobalt(Ⅲ) iodide (**12**).[28] Also, the acetyl groups were then attached as the side chains according to the X-ray crystallographic analysis of (1*S*,2*S*)-[*N*,*N*′-bis(2-acetyl-3-oxobutylidene)-1,2-bis(2,4,6-trimethylphenyl)ethylenediaminato]cobalt(Ⅲ) iodide to construct the initial structure.[29] After optimization of the transition state structure, the potential energy surface related to the rotation of the carbonyl groups was calculated to afford the transition states **13** as the most stable conformer (Fig. 10). The conformation of the carbonyl groups of the acetyl side chains and the phenyl groups on the ethylene bridge was very similar to the X-ray structure of the cobalt(Ⅲ) iodide **12**. It was found from the conformation search of the acetyl groups that the initial conformation of the acetyl group influenced the structure of the ligand plane and often resulted in an erroneous structure. The troublesome influence by the initial conformation of acetyl group increased as the system was close to the experimental system; therefore, the conformation consistent with the X-ray structure of the acetyl group was hereafter employed for the initial geometry.[30]

The methyl group was then attached to the structure **13** to complete the real cobalt complex and optimization of its structure gave the transition structure **14**. The cobalt complex involved in the structure **14** was the smallest system itself actually employed in the catalytic enantioselective cyclopropanation (Fig. 10).

Finally, the ethylene molecule was then replaced by styrene by attaching a phenyl group on the ethylene molecule. Since ethylene has four hydrogens, all the possibilities of hydrogen replacement with a phenyl group were examined. First of all, the qualitative energy potential for each replacement was calculated by rotation of the styrene around the C_c–C_1 axis. The transition state optimizations were then performed from each energy minimum of the respective potential energy surfaces to afford five transition states (Fig. 11, **15**–**19**).

As shown in Table 1, the bond formation at the β-carbon of styrene was easier than that at the α-carbon by 30 kJ mol^{-1}. Compared among the transition states structures in Fig. 11, the bonds to be newly formed at the β-carbon of styrene, C_c–C_1 and C_c–C_2, were longer while C_1–C_2 and Co–C_c were shorter

Table 1. Energies of the Transition States and Bond Forming Carbons

Entry	TS	E/kJ mol^{-1}	ΔE/kJ mol^{-1}	Bond Forming Carbon
1	**15**	−7539.1	0.0	β
2	**16**	−7535.3	3.8	β
3	**17**	−7527.6	11.5	β
4	**18**	−7508.7	30.4	α
5	**19**	−7504.9	34.2	α

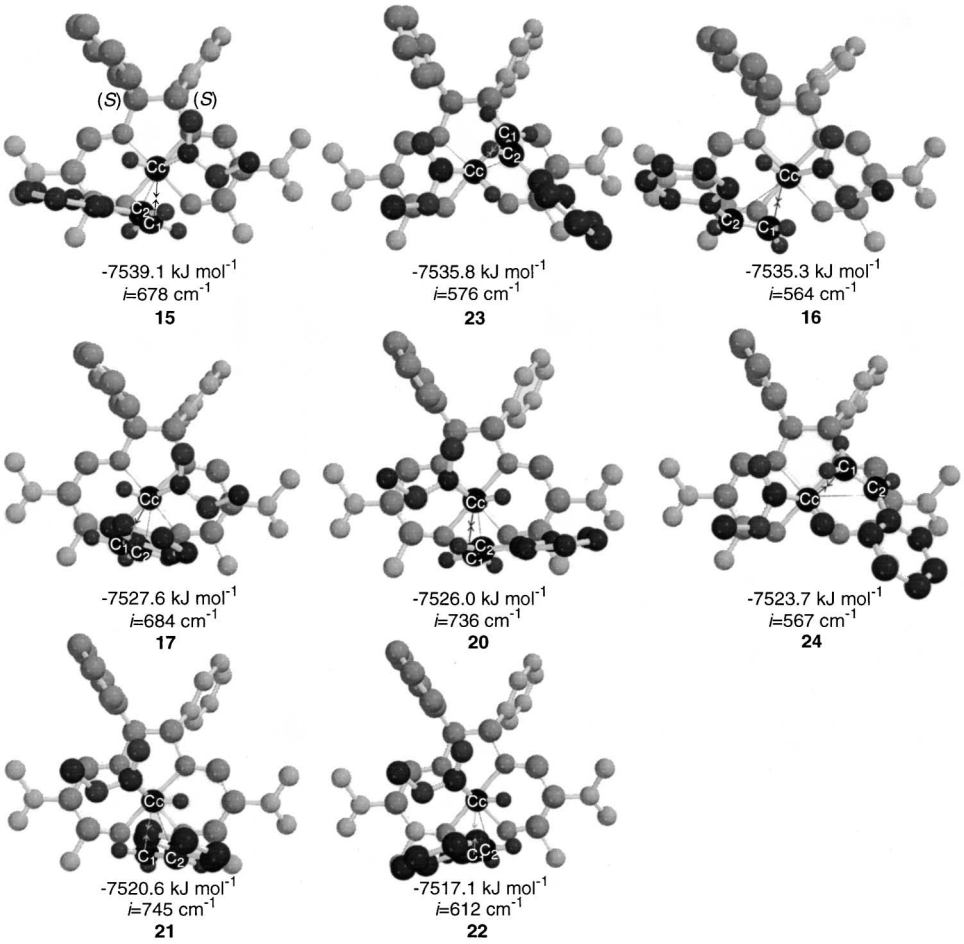

Fig. 12. Various transition states for the cobalt carbene and styrene.

than those at the α-carbon of styrene. These observations also suggested that the transition states for bond forming at the β-carbon occurred earlier than those at the α-carbon.

A density functional study and the PM3(tm) methods indicated that the ground state cobalt(II)-carbene complex was a doublet and that the spin density was mainly located on the carbene carbon. In the transition state, however, the spin density was located both on the carbene carbon and olefinic carbon apart from the bond formation. Hence, stabilization of the generated spin density by the adjacent phenyl group as well as steric reasons lead to the non-synchronous bond formation selectively at the β-carbon.[31] Based on this consideration, it is reasonable that hereafter the search of the transition state focused on the structure for the preferential bond-formation at the β-carbon of the styrene.

The chirality of the complex should next be considered. The methyl ester part in the structure **14** was converted into the mirror image by the perpendicular plane bisecting the O_1–Co–O_2 and N_1–Co–N_2 angle to prepare the enantiomeric complex model. A similar analysis for the structure was carried out using the procedure mentioned above to obtain three transition states (**20**–**22**). A trajectory analysis of the approaching olefin was finally performed on these structures. When the potential energy surfaces were calculated by rotating the fixed cyclopropane moiety around the Co–C_c axis, SCF did not converge and no reasonable energies were obtained at almost all the points because of improper initial geometries. However, two transition states were obtained after the optimization (**23** and **24**).[32]

In total, eight sets of reasonable transition states were completed (Fig. 12).

Table 2 summarizes the resulting transition states, their energies and the absolute configuration of the products in calculations. For the case when the olefin approached a perpendicular or skew orientation, the olefin should rotate clockwise or counterclockwise after the transition state to generate a cyclopropane ring structure. However, due to steric reasons, the olefin should rotate away from the ligand plane in the present reaction.

The observed features during the enantioselective cyclopropanation catalyzed by the 3-oxobutylideneaminatocobalt(II) complex are summarized and can be explained as follows:[33]

(1) (1*S*,2*S*)-*trans*-2-Arylcyclopropanecarboxylic acid ester was obtained as a major product corresponding to the (1*S*,2*S*)-cobalt(II) complex catalyst. Transition state **15** corresponding to the (1*S*,2*S*)-*trans*-product could be the most stable of the transition states listed in Table 2. The methyl ester part in the carbenoid complex should occupy the opposite site from the phenyl group in the diamine unit. Styrene could approach the carbene carbon by keeping the phenyl group away from the ester part due to the lowest steric repulsion in the transition state. Although the calculation suggested that the olefin could approach with a bisecting O_1–Co–N_1 bond like transition state

Table 2. Energies of the Transition States and Predicted Absolute Configurations of Products

Entry	TS	E / kJ mol^{-1}	ΔE / kJ mol^{-1}	*Trans* or *Cis*[a)]	Absolute Configuration[a)]
1	**15**	−7539.1	0.0	*Trans*	(1*S*,2*S*)
2	**23**	−7535.8	3.3	*Trans*	(1*S*,2*S*)
3	**16**	−7535.3	3.8	*Cis*	(1*S*,2*R*)
4	**17**	−7527.6	11.5	*Cis*	(1*S*,2*R*)
5	**20**	−7526.0	13.1	*Trans*	(1*R*,2*R*)
6	**24**	−7523.7	15.4	*Cis*	(1*S*,2*R*)
7	**21**	−7520.6	18.5	*Cis*	(1*R*,2*S*)
8	**22**	−7517.1	22.0	*Cis*	(1*R*,2*S*)

a) Predicted stereochemistries of the products corresponding to (*S*,*S*)-cobalt complex from the calculated transition-states.

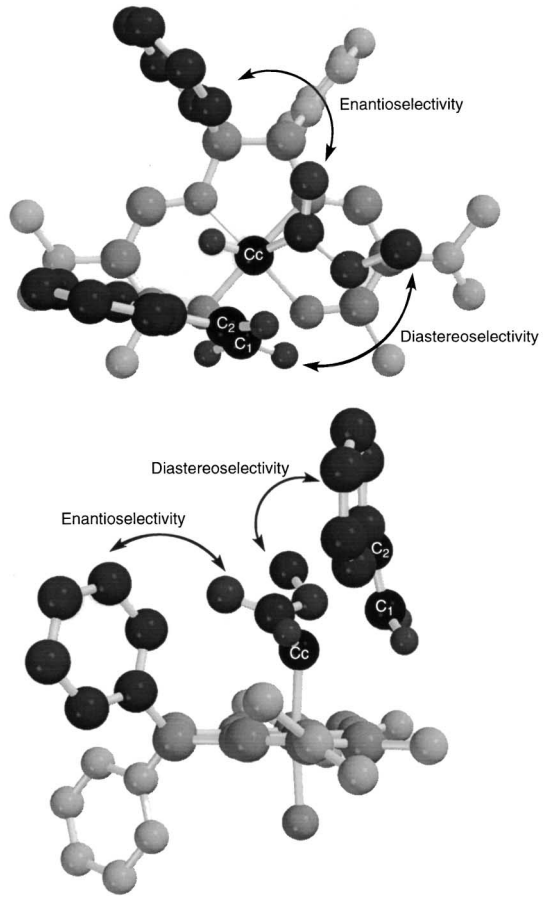

Fig. 13. Explanation of the diastereo- and enantioselectivities.

23, the more steric demanding cobalt(II) complex would make the transition state **23** more unstable compared to transition state **15** (Fig. 13).

(2) (1*S*,2*R*)-*cis*-2-Arylcyclopropanecarboxylic acid ester was obtained as a minor product corresponding to the (1*S*,2*S*)-cobalt(II) complex catalyst. Two transition states, **16** and **17**, resulted and corresponded to the *cis*-(1*S*,2*R*)-product. The olefin approached the cobalt-carbene bond in a parallel orientation in transition state **17**, but it seemed that steric repulsion between the phenyl group in styrene and the ester moiety was relatively large. On the contrary, the phenyl group in styrene was rotated to avoid the steric repulsion in transition state **16**. Based on the experimental considerations, diastereoselectivity in the present system was relatively difficult to be improved compared with the enantioselectivity. This can be explained as follows: the approaching olefin should rotate around the C_c–C_1 axis to reduce the steric repulsion, and then the activation energy for the *cis*-product decreased more than that predicted by the bulkiness of the ester part. Based on these considerations, transition state **16** was plausible for affording the *cis*-product.

(3) Enantioselectivity was enhanced as the steric demand of the ligand increased. The enantioselectivity was controlled by the orientation of the ester moiety. Steric repulsion between the diamine unit and the ester moiety increased as the steric hindrance of the diamine unit increased. Therefore, the bulky diamine unit increased the population of the ester moiety separated from the diamine unit, and it led to a decreased (1*R*,2*R*)-product via transition state **20**.

(4) The cyclopropanation of 1-phenylpropene did not proceed in the present system. 1-Phenylpropene could not approach the carbene carbon because of steric repulsion between the methyl group of the 1-phenylpropene and the ligand plane.

(5) The *trans*-selectivity disappeared in the reaction of 2-phenylpropene. It may be easily deduced from transition state **15** that a large difference in the steric size between the two substituents in the 1,1-disubstituted ethene was required for the diastereoselection. During the reaction of 2-phenylpropene, the population of transition states **15** and **17** were similar to that of styrene itself.

Conclusion

In summary, the plausible transition states consistent with the experimental results were successfully obtained by the semiempirical and density functional calculations. The enanioselectivity was regulated by the repulsion between the aryl group of the diamine unit and the ester moiety in the carbenoid complex, while the diastereoselectivity was regulated by the repulsion between the ester moiety and the approaching olefin. The present calculations provided the possibility of the analysis for the transition metal-complex-catalyzed reaction in the real system with the PM3(tm) method under the conditions that the density functional method supported the PM3(tm) method in the model system.

The authors would like to thank Prof. Warren J. Hehre of

Waventunction, Inc. for his helpful discussions during the present study, Prof. Satoshi Yabushita of Keio University for his excellent advice for the density functional calculation, and Mr. Noritaka Uchida and Ms. Miyako Takahashi of CRC, Inc., for their generous support of the PM3(tm) calculations, and Information Technology Center of Faculty of Science and Technology Keio University for their support of DFT calculation.

References

1 a) T. Aratani, Y. Yoneyoshi, and T. Nagase, *Tetrahedron Lett*., **1975**, 1707. b) T. Aratani, Y. Yoneyoshi, and T. Nagase, *Tetrahedron Lett*., **1977**, 2599. c) T. Aratani, Y. Yoneyoshi, and T. Nagase, *Tetrahedron Lett*., **1982**, 685. d) T. Aratani, *Pure Appl. Chem*., **57**, 1839 (1985).

2 a) H. Fritschi, U. Leutenegger, and A. Pfaltz, *Angew. Chem., Int. Ed. Engl*., **25**, 1005 (1986). b) H. Fritschi, U. Leutenegger, and A. Pfaltz, *Helv. Chim. Acta*, **71**, 1553 (1988). c) U. Leutenegger, G. Umbricht, C. Fahrni, P. von Matt, and A. Pfaltz, *Tetrahedron*, **48**, 2143 (1992). d) A. Pfaltz, *Acc. Chem. Res*., **26**, 339 (1993).

3 a) R. E. Lowenthal, A. Abiko, and S. Masamune, *Tetrahedron Lett*., **31**, 6005 (1990). b) D. Müller, G. Umbricht, B. Weber, and A. Pfaltz, *Helv. Chim. Acta*, **74**, 232 (1991). c) D. A. Evans, K. A. Woerpel, M. M. Hinman, and M. M. Faul, *J. Am. Chem. Soc*., **113**, 726 (1991). d) R. E. Lowenthal and S. Masamune, *Tetrahedron Lett*., **32**, 7373 (1991). e) D. A. Evans, K. A. Woerpel, and M. Scott, *Angew. Chem., Int. Ed. Engl*., **31**, 430 (1992).

4 K. Ito and T. Katsuki, *Tetrahedron Lett*., **34**, 2661 (1993).

5 a) H. Nishiyama, Y. Itoh, H. Matsumoto, S.-B. Park, and K. Itoh, *J. Am. Chem. Soc*., **116**, 2223 (1994). b) H. Nishiyama, Y. Itoh, Y. Sugawara, H. Matsumoto, K. Aoki, and K. Itoh, *Bull. Chem. Soc. Jpn*., **68**, 1247 (1995). c) S. Iwasa, F. Takezawa, Y. Tsuchiya, and H. Nishiyama, *Chem. Commun*., **2001**, 59.

6 a) M. P. Doyle, B. D. Brandes, A. P. Kazala, R. J. Poeters, M. B. Jarstfer, L. M. Watkins, and C. T. Eagle, *Tetrahedron Lett*., **31**, 6613 (1990). b) M. P. Doyle, W. R. Winchester, J. A. A. Hoorn, V. Lynch, S. H. Simonsen, and R. Ghosh, *J. Am. Chem. Soc*., **115**, 9968 (1993). c) S. Kitagaki, H. Matsuda, N. Watanabe, and S. Hashimoto, *Synlett*, **1997**, 1171.

7 a) H. M. L. Davies, P. R. Bruzinski, D. H. Lake, N. Kong, and M. J. Fall, *J. Am. Chem. Soc*., **118**, 6897 (1996). b) H. M. L. Davies, D. G. Stafford, B. D. Doan, and J. H. Houser, *J. Am. Chem. Soc*., **120**, 3326 (1998).

8 a) A. Nakamura, A. Konishi, Y. Tatsuno, and S. Otsuka, *J. Am. Chem. Soc*., **100**, 3443 (1978). b) A. Nakamura, A. Konishi, R. Tsujitani, M. Kudo, and S. Otsuka, *J. Am. Chem. Soc*., **100**, 3449 (1978). c) A. Nakamura, *Pure Appl. Chem*., **50**, 37 (1978).

9 a) T. Fukuda and T. Katsuki, *Synlett*, **1995**, 825. b) T. Fukuda and T. Katsuki, *Tetrahedron*, **53**, 7201 (1997). c) T. Niimi, T. Uchida, R. Irie, and T. Katsuki, *Tetrahedron Lett*., **41**, 3647 (2000).

10 a) T. Yamada, T. Ikeno, H. Sekino, and M. Sato, *Chem. Lett*., **1999**, 719. b) T. Ikeno, M. Sato, and T. Yamada, *Chem. Lett*., **1999**, 1345. c) T. Ikeno, A. Nishizuka, M. Sato, and T. Yamada, *Synlett*, **2001**, 407.

11 a) K. C. Brown and T. Kodadek, *J. Am. Chem. Soc*., **114**, 8336 (1992). b) J. L. Maxwell, K. C. Brown, D. Bartley, and T. Kodadek, *Science*, **256**, 1544 (1992).

12 a) M. P. Doyle, W. Hu, B. Chapman, A. B. Marnett, C. S. Peterson, J. P. Vitale, and S. A. Stanley, *J. Am. Chem. Soc*., **122**, 5718 (2000). b) M. P. Doyle and W. Ho, *J. Org. Chem*., **65**, 8839 (2000). c) M. P. Doyle, C. S. Peterson, Q.-L. Zhou, and H. Nishiyama, *Chem. Commun*., **1997**, 211.

13 T. Rasmussen, P. O. Norrby, and T. Ziegler, Abstracts of papers of the ACS (1999), 218, INOR 155.

14 a) W. J. Hehre, J. Yu, and E. Adei, Abstracts of papers of the ACS (1996), 212, COMP 092. b) W. J. Hehre, J. Yu, and P. E. A. Klunziguer, "Guide to Molecular Mechanics and Molecular Orbital Calculations in Spartan," Wavefunction, Inc., Irvine (1997).

15 Mac Spartan Pro Ver 1.0.1 and PC Spartan Pro Ver 1.0. were released from Wavefunction, Inc., 18401, Von Karman Avenue, Suite 370, Irvine, CA 92612 U.S.A.

16 J. J. P. Stewart, *J. Comp. Chem*., **10**, 221 (1989).

17 For examples, a) R. Bosque and F. Maseras, *J. Comp. Chem*., **21**, 562 (2000). b) J. Albert, R. Bosqu, J. M. Cadena, J. R. Granell, G. Muller, and J. I. Ordinas, *Tetrahedron: Asym*., **11**, 3335 (2000). c) J.Balsells, J. Vázquez, A. Moyano, M. A. Pericàs, and A. Riera, *J. Org. Chem*., **65**, 7291 (2000).

18 Gaussian 98, Revision A.6, M. J. Frisch, G. W. Trucks, H. B. Schlegel, G. E. Scuseria, M. A. Robb, J. R. Cheeseman, V. G. Zakrzewski, J. A. Montgomery, Jr., R. E. Stratmann, J. C. Burant, S. Dapprich, J. M. Millam, A. D. Daniels, K. N. Kudin, M. C. Strain, O. Farkas, J. Tomasi, V. Barone, M. Cossi, R. Cammi, B. Mennucci, C. Pomelli, C. Adamo, S. Clifford, J. Ochterski, G. A. Petersson, P. Y. Ayala, Q. Cui, K. Morokuma, D. K. Malick, A. D. Rabuck, K. Raghavachari, J. B. Foresman, J. Cioslowski, J. V. Ortiz, B. B. Stefanov, G. Liu, A. Liashenko, P. Piskorz, I. Komaromi, R. Gomperts, R. L. Martin, D. J. Fox, T. Keith, M. A. Al-Laham, C. Y. Peng, A. Nanayakkara, C. Gonzalez, M. Challacombe, P. M. W. Gill, B. Johnson, W. Chen, M. W. Wong, J. L. Andres, C. Gonzalez, M. Head-Gordon, E. S. Replogle, and J. A. Pople, Gaussian, Inc., Pittsburgh PA, 1998.

19 a) A. D. Becke, *J. Chem. Phys*., **98**, 5648 (1993). b) J. P. Perdew, *Phys. Rev. B*, **33**, 8822 (1986).

20 S.-B. Park, N. Sakata, and H. Nishiyama, *Chem. Eur. J*., **2**, 303 (1996).

21 a) N. G. Rondan, K. N. Houk, and R. A. Moss, *J. Am. Chem. Soc*., **102**, 1770 (1980). b) K. N. Houk, N. G. Rondan, and J. Mareda, *J. Am. Chem. Soc*., **106**, 4291 (1984). c) A. E. Keating, S. R. Merrigan, D. A. Singleton, and K. N. Houk, *J. Am. Chem. Soc*., **121**, 3933 (1999).

22 K. N. Houk and N. G. Rondan, *J. Am. Chem. Soc*., **106**, 4293 (1999).

23 The transition states for the perpendicular approach of ethylene could not be obtained by the DFT method, but the present method indicated that the potential energy surface for the rotation of ethylene molecule around the C_c–C_1 axis was fairly flat in the range of the dihedral angle Co–C_c–C_1–C_2 = 110–250° (Energy difference was about 4 kJ mol^{-1}). Though semiempirical calculation has a tendency to estimate the perpendicular and skew approach of ethylene slightly stable, the parallel approach of olefin was finally obtained as the most stable transition state (TS **15**). Therefore, this tendency gave little effect on the conclusion.

24 As shown in Fig. 14, totally 15 transition states were afforded as rotational isomers of transition state **8** and **9**. These isomers were obtained by rotating cyclopropane moiety around the Co–C_c bond and ethylene around the C_c–C_1 as an axis (Fig. 14).

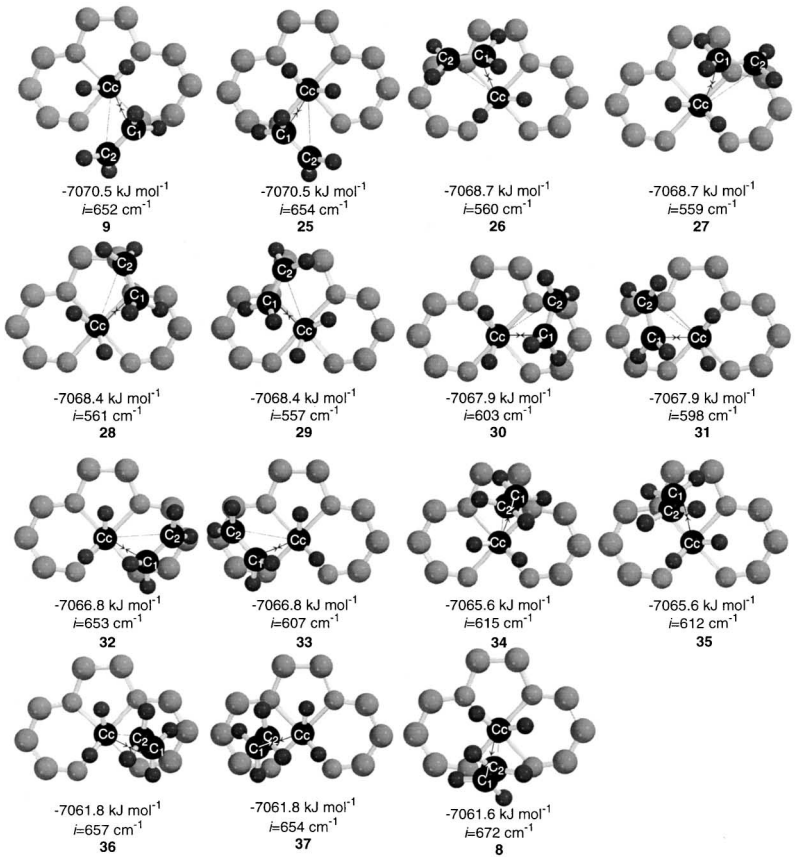

Fig. 14. Various transition states of the reaction between the model complex **6** and ethylene.

25 Concerned with a rotational isomer of methoxycarbonyl moiety, for example, the transition state **38** was obtained corresponding to the transition state **11**. Although the transition state **38** ($E = -7436.3$ kJ mol^{-1}) was more stable than the transition state **11** ($E = -7433.0$ kJ mol^{-1}), the phenyl groups attached to the ethylene bridge in the real experimental system should destabilize the structure **38** because of the steric repulsions. Therefore, it is plausible to adopt structure-**11**-type orientation of methoxycarbonyl group as a basic orientation (Fig. 15).

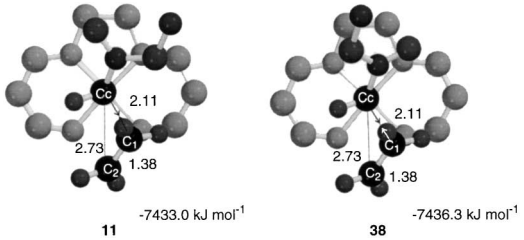

Fig. 15. Transition states for the reaction of the cobalt carbene complex with ethylene at PM3(tm).

26 Nine rotational isomers were shown in Fig. 16.

27 To explain clearly, phenyl and acetyl groups were attached to the transition state **11** as a representative model. Any rotational isomers can be used for initial geometries and the same results were obtained.

28 T. Yamada, T. Nagata, T. Ikeno, Y. Ohtsuka, A. Sagara, and T. Mukaiyama, *Inorg. Chim. Acta*, **296**, 86 (1999).

29 S. Ohba, T. Nagata, and T. Yamada, *Acta Crystallogr.*, **E57**, m124 (2001).

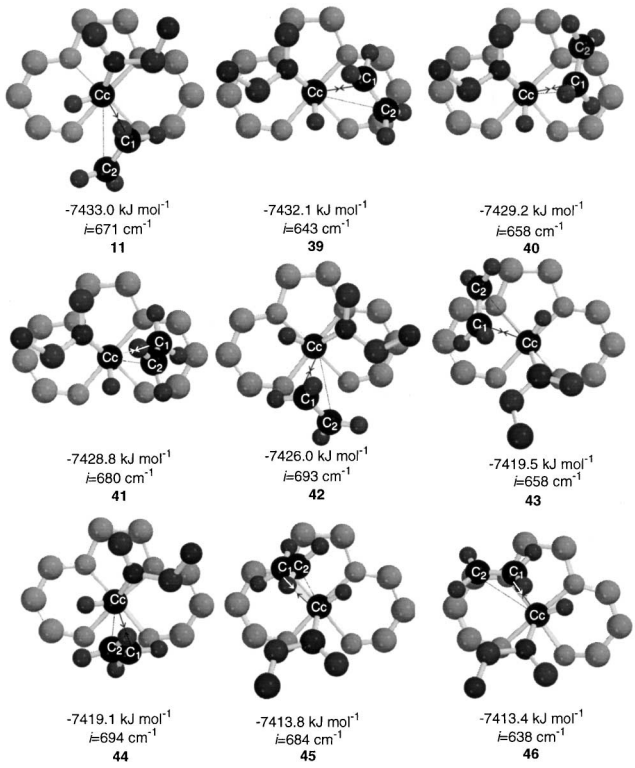

Fig. 16. Various transition states of the reaction between the cobalt carbene complex and ethylene.

30 Direct analyses of the present cyclopropanation in real experimental system by the PM3(tm) method were very complicated, because the usual conformation search was not reliable. Too many unreasonable structures were obtained in such a large system and a slight difference in initial geometry often lead to different optimized structures. Therefore, it was required that the analyses started from a simple model system and developed into a real experimental system by step by step checking the validity of the afforded structures.

31 Since the carbene carbon of the cobalt(II) carbene complex possessed a radical character, the initial bond formation preferentially occurred at the terminal carbon of styrene. Similar radical character was proposed in the salen-Mn catalyzed epoxidation by the density functional method, and it was indicated that the stereoselectivity was dominated at the initial carbon–oxygen bond formation step. L. Cavallo and H. Jacobsen, *Angew. Chem., Int. Ed. Engl.*, **39**, 589 (2000).

32 Unreasonable transition states were omitted.

33 See the preceding paper.